USGS
science for a changing world

Prepared in cooperation with Portland General Electric

Fish Behavior and Abundance Monitoring Near a Floating Surface Collector in the North Fork Reservoir, Clackamas River, Oregon, Using Multi-Beam Acoustic Imaging Sonar

Open-File Report 2018–1182

U.S. Department of the Interior
U.S. Geological Survey

Cover: Photograph showing North Fork Dam and the floating surface collector on the Clackamas River, Oregon, June 24, 2015. Photograph by Portland General Electric. Used with permission.

Fish Behavior and Abundance Monitoring Near a Floating Surface Collector in North Fork Reservoir, Clackamas River, Oregon, Using Multi-Beam Acoustic Imaging Sonar

By Collin D. Smith, John M. Plumb, and Noah S. Adams

Prepared in cooperation with Portland General Electric

Open-File Report 2018-1182

U.S. Department of the Interior
U.S. Geological Survey

U.S. Department of the Interior
RYAN K. ZINKE, Secretary

U.S. Geological Survey
James F. Reilly II, Director

U.S. Geological Survey, Reston, Virginia: 2018

Suggested citation:
Smith, C.D., Plumb J.M., and Adams, N.S. 2018, Fish behavior and abundance monitoring near a floating surface collector in North Fork Reservoir, Clackamas River, Oregon, using multi-beam acoustic imaging sonar: U.S. Geological Survey Open-File Report 2018-1182, 28 p., https://doi.org/10.3133/ofr20181182.

ISSN 2331-1258 (online)

Contents

Abstract 1
Introduction 2
Methods 4
  Dam Operations and Environmental Conditions 4
  Imaging Sonars 4
    Surveillance System 4
    Data Collection 5
    Data Processing 5
    Data Analysis 6
    Fish Size and Count 6
    Direction of Fish Travel 6
    Track Characteristics 7
    Evaluating the Fish Track Density near the Floating Surface Collector Entrance 7
  Modeling Predators and Smolts in Front of the Floating Surface Collector 7
Results 9
  Definition of Study Period 9
  Dam Operations and Environmental Conditions 9
  Fish Abundance 11
  Direction of Travel 12
  Fish Tortuosity and Swimming Velocity 15
  Timing of Detection 17
  Spatial Fish Distribution 17
  Model Selection and Fit 19
    Factors Affecting the Counts of Predators 20
Discussion 23
Acknowledgments 25
References Cited 25

Figures

Figure 1. Graphic showing Clackamas River Basin showing North Fork Reservoir and Dam, Oregon 2
Figure 2. Orthoimage showing floating surface collector at North Fork Dam, Oregon, 2017 3
Figure 3. Photograph of North Fork Reservoir floating surface collector and approximate coverage area of the ARIS® imaging sonar (red cone) in forebay of North Fork Reservoir, Oregon, 2017 5
Figure 4. Graph of Clackamas River discharge at U.S. Geological Survey hydrological site 14210000 located at Estacada, Oregon, April 19–June 1, 2017 10
Figure 5. Graph showing project and spillway discharge and reservoir elevation at North Fork Dam, Oregon, April 19–June 1, 2017 10
Figure 6. Graph showing turbidity and water temperature at North Fork Dam, Oregon, April 19–June 1, 2017 11
Figure 7. Graph showing daily count of fish on the date of detection using the ARIS® imaging sonar at the floating surface collector at North Fork Reservoir, Oregon, 2017 12
Figure 8. Rose diagram of mean travel directions (in degrees) for smolt-size fish detected using the ARIS® imaging sonar outside the floating surface collector at North Fork Reservoir, Oregon, 2017 13

Figure 9. Rose diagram of mean travel directions (in degrees) for predator-size fish detected using the ARIS® imaging sonar outside the floating surface collector at North Fork Reservoir, Oregon, 2017 14
Figure 10. Diagram of directional travel for smolt-size fish detected in the presence or absence of predator-size fish using the ARIS® imaging sonar outside the floating surface collector at North Fork Reservoir, Oregon, 2017 15
Figure 11. Boxplots of the tortuosity index and swimming velocity of fish observed with ARIS® imaging sonar near the entrance to the floating surface collector in the North Fork Reservoir, 2017..... 16
Figure 12. Graph showing count of fish by hour of detection using the ARIS® imaging sonar at the floating surface collector at North Fork Reservoir, Oregon, April 19–June 1, 2017 17
Figure 13. Graph showing the location point density for smolt-size fish detected using the ARIS® imaging sonar outside of the entrance to the floating surface collector at North Fork Reservoir, Oregon, April 19–June 1, 2017..... 18
Figure 14. Graph showing the location point density for predator-size fish detected using the ARIS® imaging sonar outside of the entrance to the floating surface collector at North Fork Reservoir, Oregon, April 19–June 1, 2017..... 19
Figure 15. Graph showing the probability of zero-inflation by smolt-size fish abundance and day and night effects for the zero-inflation Poisson model of hourly predator-size fish counts near the entrance to the floating surface collector at North Fork Reservoir, Oregon 22
Figure 16. Graphs showing the influence of smolt-size fish abundance by day and night for the zero-inflation Poisson model of hourly predator-size fish counts near the entrance to the floating surface collector at North Fork Reservoir, Oregon. 23

Tables

Table 1. Summary statistics of hourly dam operations and environmental conditions at North Fork Dam, Oregon, April 19–June 1, 2017. 11
Table 2. Mean travel directions and concentration parameter for fish observed using the ARIS® imaging sonar outside of the floating surface collector at North Fork Reservoir, Oregon, 2017. 12
Table 3. Summary statistics for the tortuosity and swimming velocity of fish observed using the ARIS® imaging sonar outside the floating surface collector at North Fork Reservoir, Oregon, 2017. 16
Table 4. Model selection results showing the model, the number of parameters, Akaike's Information Criterion, and the change in AIC from the AIC lowest model (model 2). 21
Table 5. Parameter estimates and summary statistics for the zero-inflation Poisson model of hourly predator-size fish counts near the entrance to the floating surface collector at North Fork Reservoir, Oregon..... 22

Conversion Factors

U.S. customary units to International System of Units

Multiply	By	To obtain
	Length	
foot (ft)	0.3048	meter (m)
	Area	
acre	4,047	square meter (m^2)
acre	0.4047	hectare (ha)
acre	0.4047	square hectometer (hm^2)
	Volume	
gallon (gal)	3.785	liter (L)
gallon (gal)	0.003785	cubic meter (m^3)
acre-foot (acre-ft)	1,233	cubic meter (m^3)
acre-foot (acre-ft)	0.001233	cubic hectometer (hm^3)
	Flow rate	
foot per second (ft/s)	0.3048	meter per second (m/s)
cubic foot per second (ft^3/s)	0.02832	cubic meter per second (m^3/s)

International System of Units to U.S. customary units

Multiply	By	To obtain
	Length	
centimeter (cm)	0.3937	inch (in.)
millimeter (mm)	0.03937	inch (in.)
meter (m)	3.281	foot (ft)
kilometer (km)	0.6214	mile (mi)
kilometer (km)	0.5400	mile, nautical (nmi)
	Area	
hectare (ha)	2.471	acre
	Volume	
liter (L)	0.2642	gallon (gal)
	Flow rate	
meter per second (m/s)	3.281	foot per second (ft/s)
	Mass	
milligram (g)	0.000035	ounce, avoirdupois (oz)

Temperature in degrees Celsius (°C) may be converted to degrees Fahrenheit (°F) as:

$$°F = (1.8 \times °C) + 32.$$

Datums

Vertical coordinate information is referenced to the National Geodetic Vertical Datum of 1929 (NGVD 29).
Elevation, as used in this report, refers to distance above the vertical datum.

Supplemental Information

Concentrations of chemical constituents in water are given in either milligrams per liter (mg/L).

Abbreviations

AIC	Akaike Information Criterion
ANOVA	analysis of variance
ARIS®	adaptive resolution imaging sonar
CL	confidence limit
CSV	comma-separated values
FSC	floating surface collector
IQR	interquartile range
NOAA	National Oceanic and Atmospheric Administration
NTU	Nephelometric turbidity unit
PGE	Portland General Electric
Project	Clackamas River Hydroelectric Project
SD	standard deviation
SE	standard error
USGS	U.S. Geological Survey
ZIP	zero-inflated Poisson

Fish Behavior and Abundance Monitoring Near a Floating Surface Collector in North Fork Reservoir, Clackamas River, Oregon, Using Multi-Beam Acoustic Imaging Sonar

By Collin D. Smith, John M. Plumb, and Noah S. Adams

Abstract

An imaging sonar was used to assess the behavior and abundance of fish sized the same as salmonid smolt and bull trout (*Salvelinus confluentus*) at the entrance to the juvenile fish floating surface collector (FSC) at North Fork Reservoir, Oregon. The purpose of the FSC is to collect downriver migrating juvenile salmonids (Chinook salmon [*Oncorhynchus tshawytscha*], Coho salmon [*Oncorhynchus kisutch*], and steelhead [*Oncorhynchus mykiss*]) at the North Fork Dam and to safely route them around the hydroelectric projects. The objective of the imaging sonar component of this study was to assess the behaviors of both smolt and predator-size fish (smolt [60–250 millimeter] and predator 350–650 [millimeter]) observed near the FSC and to determine if the presence of predator-size fish influenced the abundance of smolt-size fish. An imaging sonar was deployed near the entrance to the FSC during the spring smolt out-migration period. The imaging sonar technology was an informative tool for assessing abundance and spatial and temporal behaviors of both smolt and predator-size fish near the entrance of the FSC. Both smolt and predator-size fish were regularly observed near the entrance, with greater abundances observed during day than during night. Behavioral differences were also observed between the two fish-size classes, with smolt-size fish traveling straighter with more directed movement, and predator-size fish generally showing more milling behavior. Additionally, the presence of predator-size fish may be effecting the abundance and direction of travel of smolt-size fish, as counts of smolt-size fish were reduced in conjunction with the presence of predator-size fish and a greater proportion of smolt-size fish were observed traveling away from the FSC when predator-size fish were present than when predator-size fish were absent. Results of modeling potential predator-prey interactions and influences indicated that both the number of juvenile fish tracks and photoperiod had the strongest effects on the number of predator fish tracks, with more predator-size fish tracks observed as the number of smolt-size fish tracks increased. Overall, the results indicate that predator-size fish are present near the entrance of the FSC, concomitant with smolt-size fish, and their abundances and behaviors indicate that they may be drawn to the entrance of the FSC because of the abundance of prey-sized fish found there.

Introduction

Portland General Electric (PGE) operates the Clackamas River Hydroelectric Project (Project) in northwestern Oregon, which includes a series of powerhouses, dams, reservoirs, and support facilities (fig. 1). The primary purpose of the Project is hydroelectric power generation, but it also is operated to provide flood-risk management, along with water for instream flows for wildlife and opportunities for recreation. In 2008, the National Oceanic and Atmospheric Administration (NOAA) determined that the Project was a limiting factor for upstream and downstream fish passage of anadromous fish stocks in the Clackamas River Basin and mandated a series of Project improvements (National Oceanic and Atmospheric Administration, 2008).

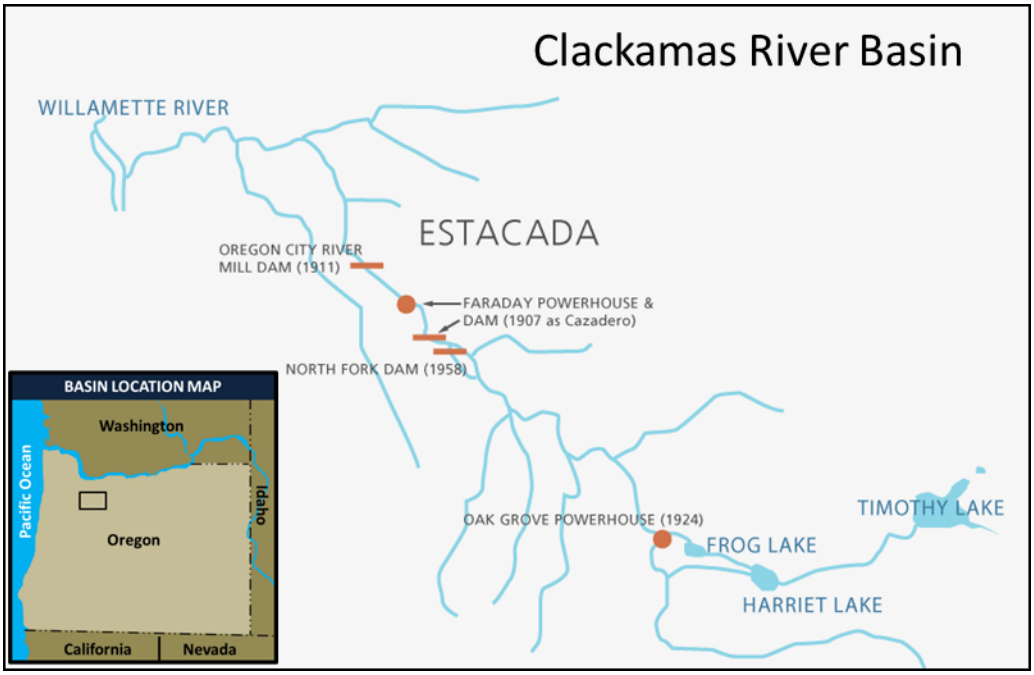

Figure 1. Graphic showing Clackamas River Basin showing North Fork Reservoir and Dam, Oregon. Graphic from Portland General Electric.

North Fork Dam is a 63-m-high, thin-shell concrete arch dam on the Clackamas River about 48 km southeast of Portland. The dam, completed in 1958, is owned and operated by PGE. It has a hydraulic capacity of 6,000 cubic feet per second (ft^3/s) and two Francis turbine units capable of generating a total of 60 megawatts. During normal operations, all water passing through the dam goes through the powerhouse located in the center of the dam (fig. 2), with the exception of a continuous 43 ft^3/s flow that maintains a 3.1-km-long fishway along the northern side of the dam and along the Clackamas River. A spillway with three Tainter gates is on the northern side of the dam but is not used during normal dam operations. The 331-acre North Fork Reservoir created by the dam has a storage capacity of 18,630 acre-ft, and a useable storage capacity of 700 acre-ft. The forebay elevation typically fluctuates ±2 ft during normal weather and project operations.

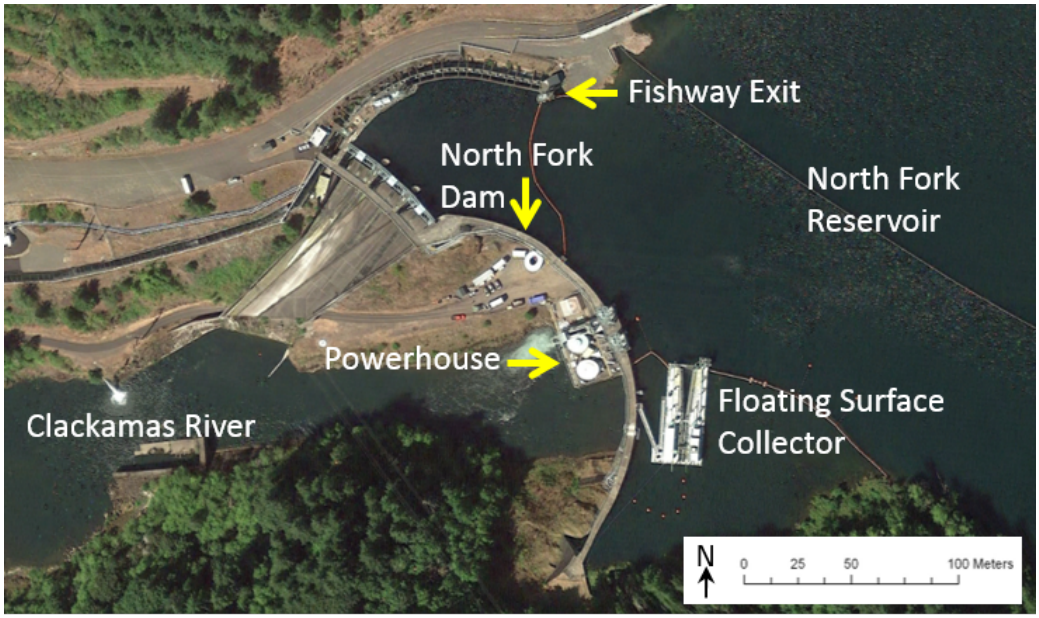

Source: Landsat 8/11/2016

Figure 2. Orthoimage showing floating surface collector at North Fork Dam, Oregon, 2017.

The juvenile bypass facility at North Fork Dam was marginally effective at passing salmonid smolts migrating downriver (Federal Energy Regulatory Commission, 2006). The 2008 finding by NOAA spurred the construction of a floating surface collector (FSC) with the goal of improving downstream passage of salmonid smolts at North Fork Dam by collecting fish near the dam and moving them downstream. Surface collection has been shown to be a viable method of attracting salmonid smolts (Sweeney and others, 2007), and floating surface collectors have been used at several high-head dams in the Pacific Northwest, including Upper Baker Lake (National Oceanic and Atmospheric Administration, 2018). As a result of successes at Upper Baker Lake and elsewhere, a FSC was installed in North Fork Reservoir during spring 2015 and evaluated for hydraulic performance throughout much of that year (Christensen and Grant, 2015).

The FSC is about 20 × 45 m in size and uses pumps to draw water from the reservoir with a maximum inflow of 1,000 ft^3/s and a minimum capture velocity of 6.3 feet per second (ft/s). Fish are guided toward the collector flume (5 m wide × 5.9 m deep) with the use of guidance nets, enter the flume, move past dewatering screens, and then pass directly into a bypass pipe that delivers them into the tailrace of River Mill Dam about 8.2 km downriver. The entrance of the FSC is placed near the center of the reservoir and near the turbine intakes, as fish tended to congregate along the dam, and the dam could be used to congregate and guide fish toward the flume of the FSC. Additional information on FSC operations and performance may be found in Ackerman and Pyper (2017); Ackerman and others (2017); and Wyatt (2017).

As part of the evaluation to determine how well the FSC performs at collecting and passing salmonid smolts, there is a need to assess the potential effect that the presence of predatory fish may have on the efficacy of the structure. Reintroductions of bull trout (*Salvelinus confluentus*) recently have been implemented in the Clackamas River subbasin (U.S. Fish and Wildlife Service and Oregon Department of Fish and Wildlife, 2011; Barry and others, 2014), where they previously had been believed to be extirpated (Shively and others, 2007). As part of this reintroduction project, a total of 2,835 bull trout have been released into the Clackamas River basin between 2011 and 2016 (Barrows and others, 2017). Bull trout are known to inhabit the reservoir where the FSC is located, and they are known predators of juvenile salmonids. In addition to bull trout, rainbow trout (*Oncorhynchus mykiss*) are the only other known predators of salmonid smolts present in the reservoir, and also could potentially be observed with the imaging sonar. We used an imaging sonar to determine if predator-size fish are present near the collector and to determine if they are interacting with smolt-size fish as they approach the entrance, thereby preventing them from entering and subsequently reducing the number of juvenile salmonids passing into the FSC and ultimately reducing overall collection efficiencies.

The study summarized in this report was designed to provide empirical information about the presence, movement, and behaviors of both smolt and predator-size fish near the entrance to the FSC, as well as the potential predator-prey interactions at the FSC, to help inform decisions about collection and passage solutions. Measures of the biological performance were quantified using imaging sonar based on the abundance and behaviors of fish near the FSC. The study was designed to provide information for the following objectives:

- To quantify the spatial and temporal distribution and overlap of smolt and predator-size fish near the entrance of the FSC;
- To assess how the hourly count of juvenile fish tracks, photoperiod, water clarity, and river flow may influence the number of predators in front of the FSC.

Methods

Dam Operations and Environmental Conditions

Project discharge, spillway discharge, reservoir elevation, and water temperature data were summarized to document the environmental conditions that fish experienced from April 19 to June 1, 2017. Hourly powerhouse discharge and reservoir elevation data were provided by PGE. Turbidity and water temperature data were collected at the U.S. Geological Survey (USGS) streamgage on the Clackamas River at Estacada, Oregon, and obtained at U.S. Geological Survey (2018). Data were summarized using hourly observations, but mean daily values were plotted to increase clarity in the plots. Water elevation data are presented in feet and discharge is presented in cubic feet per second (ft^3/s) according to the local convention.

Imaging Sonars

Surveillance System

We used an adaptive resolution imaging sonar (ARIS®) to collect data on fish movements. The ARIS® imaging sonar was operated at 1.8 MHz, with a blanking distance of about 3 m from the camera and a maximum range of about 14 m. The camera was attached to a pole-mounted platform on the western side of the collectors entrance and aimed perpendicular (west to east) to the entrance of the collector (fig. 3). The sonar was lowered to a depth of 1.2 m below water surface and deployed on a rotator to provide precise aiming.

Figure 3. Photograph of North Fork Reservoir floating surface collector and approximate coverage area of the ARIS® imaging sonar (red cone) in forebay of North Fork Reservoir, Oregon, 2017. Photograph by Landsat, August 11, 2016.

Data Collection

The imaging sonar collected data continuously at the entrance of the FSC between April 19 and June 1, 2017, to coincide with the presence of smolts. Data collection was interrupted only when the sonar was repositioned to maximize fish approach viewing or when equipment malfunctioned. All data collected were stored to hard drives for archival and subsequent processing.

Data Processing

Signal processing of the raw acoustic signals collected with the ARIS® imaging sonar was analyzed using Echoview® software (version 5.4, Myriax Pty., Ltd., Hobart, Tasmania, Australia). The software is a visualization and analysis program for hydroacoustic data. The Echoview® platform allows the operator to use successive filters to manipulate data to enhance the acoustic signal and remove static objects and noise from acoustic returns (Kang, 2011). Non-stationary acoustic returns are identified as

targets within individual camera frames and converted to three-dimensional position and time data that can then be applied to target tracking, which is used to obtain counts and movements of individual fish, along with their associated behavioral and morphometric data (Simmonds and MacLennan, 2005). Unfiltered video footage was observed congruently with tracking of the processed acoustic signals during target tracking to ensure that only fish targets were included in the dataset and target morphometric data was concomitant with target data observed in the video footage. The operational steps used for processing acoustic signals may be found in Adams and Smith (2017).

Data Analysis

Summary statistics of fish targets derived from Echoview® (for example, mean length, direction, speed, tortuosity, angle, orientation) were imported into SAS (SAS System for Windows, version 9.3, SAS Institute, Inc., Cary, North Carolina), for subsequent proofing and to merge imaging sonar data with the environmental data. Data were proofed to eliminate non-valid records or records that did not provide measurable morphometric or behavioral data. To consider a fish track as valid, we required that each fish track consisted of at least five pings and had a minimum duration of detection of 0.5 seconds. Target datasets were then exported as comma-separated values files for statistical analysis.

It is important to remember the limitations associated with data collected with imaging sonar. For instance, there is no way to identify the species of fish, especially if they are of similar size, and the imaging sonar technology cannot distinguish fish that have entered and exited the field of view multiple times; therefore, the detection duration for each individual fish track within a camera beam was determined by the time a fish was first detected by the camera to the time that the fish exited the camera view.

Fish Size and Count

Fish targets were grouped into three size classes to distinguish between smolt-size fish (60–250 mm), predator-size fish (350–650 mm), and upriver-migrating adult salmonids (>650 mm), which included steelhead and coho salmon that entered the reservoir through the fishway. The fish-size thresholds are based on measurements of juvenile salmonid outmigrants collected by the FSC, bull trout collected at the FSC or observed in the fishway, and upriver-migrating adult salmonids observed in the fishway (Garth Wyatt, Portland General Electric, oral commun., 2017). Although they were retained, data for fish 250–350 mm and greater than 650 mm were not included in this analysis.

Direction of Fish Travel

To summarize the directions of fish traveling near the FSC, we implemented circular statistics to calculate modes and measures of variability (Mardia and Jupp, 2000) using the circular package for R software (R Core Team, 2014). Tests for randomness were performed to determine if the sample population presented either uniform (random) or directed travel paths. If the data were shown to conform to a Von Mises distribution (Zar, 1999; Pewsey and others, 2013), the Rayleigh z test was performed. Data that were multi-modal or did not follow a Von Mises distribution were subjected to the Rao's spacing test (Batschelet, 1981). If the P-value was significant (at the α=0.05 level), then it was assumed that the direction of fish travel was non-random. Additionally, we used a Chi-square test to determine if the presence of predator-size fish significantly influenced (at the α=0.05 level) the abundance and general direction of travel (toward or away from the FSC) of smolt-size fish.

Track Characteristics

Fish-track characteristics were quantified using travel speed and tortuosity variables exported from Echoview®. Travel speed was calculated as the average travel velocity of each individual target. A tortuosity index (τ) was calculated as adapted from Johnson and Moursund (2000):

$$\tau = \left(\frac{\text{Sum of Length of a Track}}{\text{Straight Line Track Distance}} \right) \quad (1)$$

Applying this calculation of tortuosity, a fish traveling in a straight line will have a tortuosity index of 1.0, whereas a fish traveling in a non-linear path will have a tortuosity index of greater than 1.0.

For each of the fish track characteristics, an analysis of variance (ANOVA) was used to determine the significance of the differences for fish sizes. Statistical analyses were carried out using R software (R Core Team, 2014). A significance level of α=0.05 was used for all tests.

Evaluating the Fish Track Density near the Floating Surface Collector Entrance

The collected point samples for each individual fish track were used to create two-dimensional density plots of unique fish track locations for the volume sampled. The spatial resolution within the view of the camera was about 1 cm, and interpolation of point data was performed using the "akima" package for R software (R Core Team, 2014). The magnitude of the point count is defined as the count of unique observations of each individual fish location within each cell. Datasets for each fish size were used for plotting point location data.

Modeling Predators and Smolts in Front of the Floating Surface Collector

To quantify factors affecting the presence of predator-size fish in front of the FSC, we tabulated the number of tracks by predator and smolt-size fish for each hour of sonar footage. We fit a zero-inflated Poisson (ZIP) model to the count data using the "pscl" package and R software (R Core Team, 2014). We chose this modeling approach because of the high frequency of zeros in the dataset, which might be expected given that the sonar sampled a relatively small area upstream of the dam (Zuur and others, 2009). For example, of the 792 hours of camera footage, 78 hours (10 percent of the data) had no predator-size fish counted within the acoustic beam. Given a Poisson distribution, the sample size, and the observed mean number of predator-size fish tracks, we estimated that less than 1 percent of the hourly data should have had zero values. Thus, the high frequency of zeros prompted us to use a zero-inflated Poisson model to assess the factors affecting the absence, and conversely the occurrence and count of predator-size fish tracks upstream of the FSC.

The ZIP model consists of two sub models a Poisson model for the count of predators (that is, number of observations in an hour) and a zero-inflation model for the probability of observing an extra zero (that is, predator-size fish are absent) in front of the FSC over and above that expected under the Poisson distribution. Our Poisson count model for the number of tracks for predator-size fish per hour (B) may be expressed as

$$\log(\hat{B}_t) = \beta_0 + \sum \beta_n X_{n,t} \quad , \tag{1}$$

where

β_0 is the intercept,

β_n are the n coefficients for the X_n set of covariates, and assumes that the number of hourly tracks by the predators upriver of the FSC ($\hat{B}_t$) are Poisson distributed, whereby the mean is equal to the variance.

Our full model included covariates: (1) the square root of the hourly number of smolt-size fish tracked in the sonars' beam, (2) the photoperiod (day versus night), (3) water turbidity in Nephelometric turbidity units (NTUs), and (4) the total river discharge. We defined day time (1) between 0600 and 1759 and nighttime (0) between 1800 and 0559. Preliminary analyses indicated that a square root transformation was required to linearly transform the relation between the hourly count of predator and smolt-size fish tracks. The hourly number of smolt-size fish tracks ranged from 0 to 1,076, with a mean of 44.9 (sd=77.2). We standardized water turbidity and total river flow in the model to aid in estimation and parameter interpretation. Preliminary model diagnostics revealed low variance inflation factors (<2.65), indicating that collinearity among the covariates was not likely to be a problem. Additional environmental covariates of reservoir elevation and water temperature were included in preliminary analyses, but these variables did not contribute significantly to warrant inclusion in formal model selection.

In addition to modeling the hourly count of predator-size fish tracks, the ZIP model accounted for the amount of "extra" zeros observed in the acoustic beam in front of the FSC. Although these extra zeros may be the result of sampling a relatively small area (Zuur and others, 2009), they may also arise from environmental conditions that can affect the absence and conversely presence of predator-size fish in front of the FSC. Our zero-inflation model used a logit link function that can be expressed as

$$\hat{Z}_t = \text{logit}^{-1}(\alpha_0 + \sum \alpha_n X_{n,t}) , \tag{2}$$

where

α_0 is the intercept, and

α_n are the coefficients for the X_n set of covariates.

The model assumes that the frequency of extra zeros ($\hat{Z}_t$) follows a binomial distribution. We used the same set of covariates to model the zero-inflation as in the Poisson count model discussed above.

We used Akaike's Information Criterion (AIC) to judge the fit of candidate model subsets to the data over a range of model subsets extending from a null model (intercepts only) to a full model where all covariates are used to explain variation in the count and zero-inflation of predator-size fish tracks upstream of the FSC (Akaike, 1973; Burnham and Anderson, 2002; Zuur and others, 2009). We used a two-stage model selection process, whereby variables important to zero-inflation were evaluated first, and then using this "best" zero-inflation model we evaluated the variables important to the Poisson distributed counts. Our candidate model subsets of the zero-inflation and count models were chosen using a simple step-wise backwards removal procedure, whereby individual variables were dropped from the full model and the relative change in AIC value was used to determine the relative importance of the variable to the model. We evaluated 16 candidate models: a null, or intercept-only model having no covariates, and a full model of all covariates. Our candidate model set did not exhaustively compare all possible model subsets, the candidate models evaluated were based on logical assumptions about predator and prey relationships, and were sufficient in determining the relative importance of the factors that might affect the absence (zero-inflation), presence, and number (count) of predator-size fish at the entrance to the FSC. When interpreting the results it is important to keep in mind that the imaging sonar cannot distinguish individual fish, and so the number of tracks does not equal the abundance of fish in front to the FSC, but rather is the result of both higher fish abundance as well as fish activity, and so the count of fish tracks per hour reflects both the number and activity of predator or smolt-size fish in the vicinity of the FSC.

Results

Definition of Study Period

The period for imaging sonar data analysis includes dates between April 19 and June 1, 2017, to coincide with the peak outmigration timing of juvenile coho salmon and steelhead. Data collection was interrupted only when the sonar was repositioned or underwent general maintenance, or when equipment malfunctioned. During this time period, 34 dates with complete data files for each 24-h period were included in the analysis.

Dam Operations and Environmental Conditions

Higher than average rainfall and snowmelt resulted in greater instream flows on the Clackamas River than are normally experienced during the typical spring seasonal pattern (fig. 4). Project discharge throughout the study period closely coincided with river flows (fig. 5). Mean hourly project discharge was 5,292.4 ft^3/s (range 2,948.0–8,654.5 ft^3/s; table 1). The spillway was opened three times during the study to allow water from excess rainfall and snowmelt to pass the project, with a peak spillway discharge of 2,394.8 ft^3/s occurring on April 27, 2017. The reservoir elevation was maintained at a constant daily elevation of nearly 665 feet above National Geodetic Vertical Datum of 1929 (NGVD 29) for the entirety of the study, with a 0.3-ft fluctuation. Increases in water turbidity throughout the study period also coincided with river flows (fig. 6). The mean turbidity was 1.7 NTU's (range 0.7–4.3 NTU's). Water temperature generally increased through the study period, with a peak at 11.9 °C on May 31, 2017, whereas the minimum water temperature of 6.3 °C occurred on April 29, 2017. The FSC and the fishway operated uninterrupted during the entirety of this study.

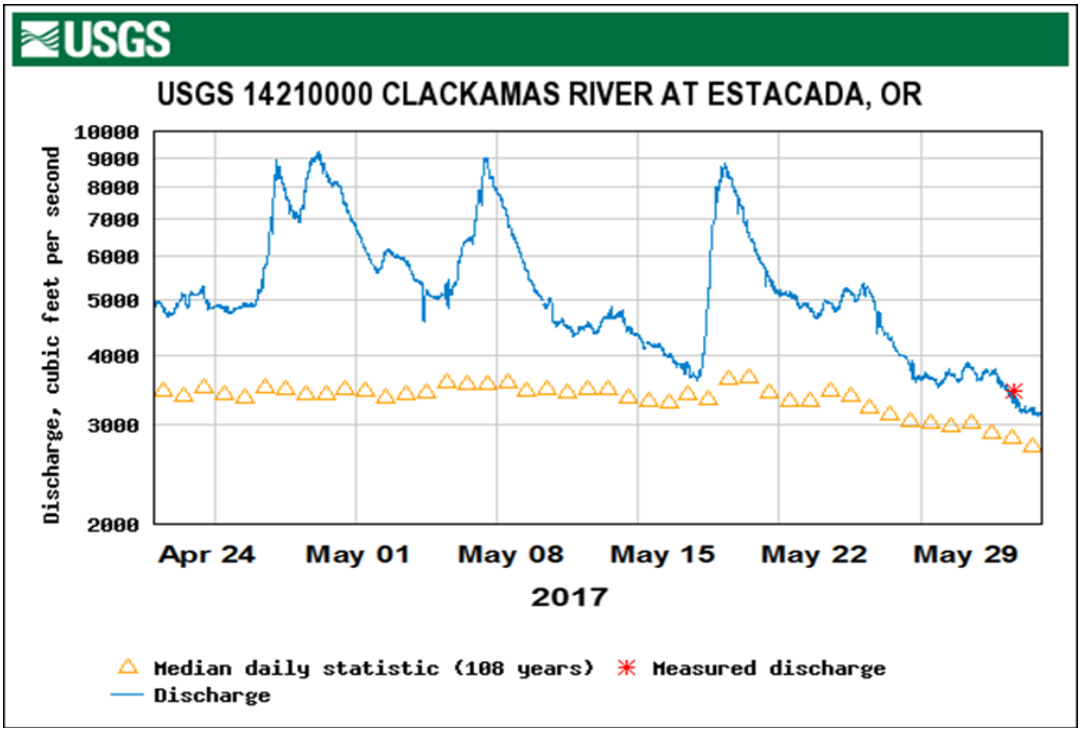

Figure 4. Graph of Clackamas River discharge at U.S. Geological Survey hydrological site 14210000 located at Estacada, Oregon, April 19–June 1, 2017. Graph produced from data at U.S. Geological Survey (2018).

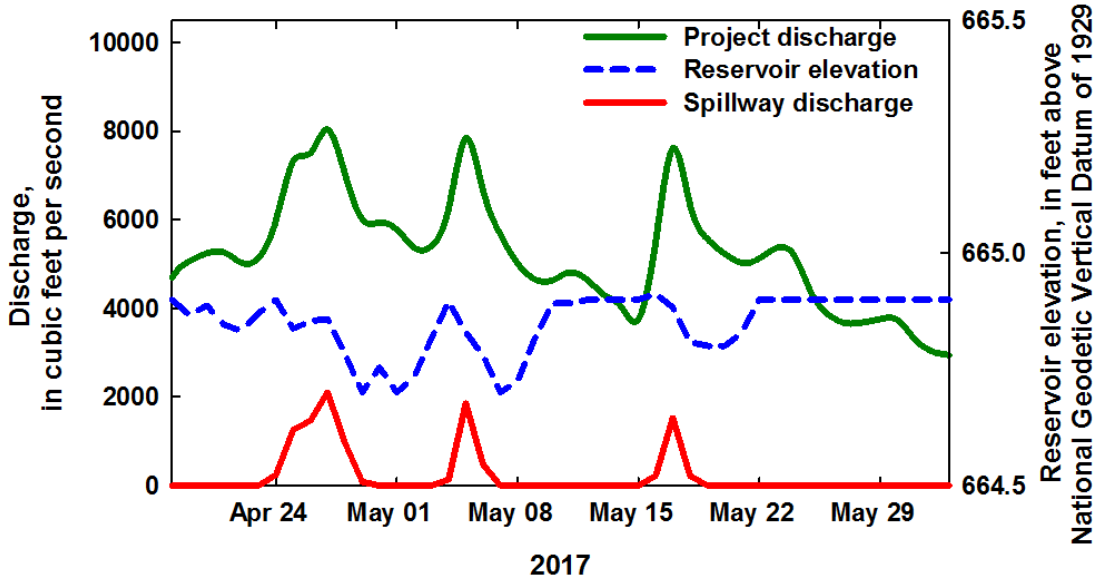

Figure 5. Graph showing project and spillway discharge and reservoir elevation at North Fork Dam, Oregon, April 19–June 1, 2017.

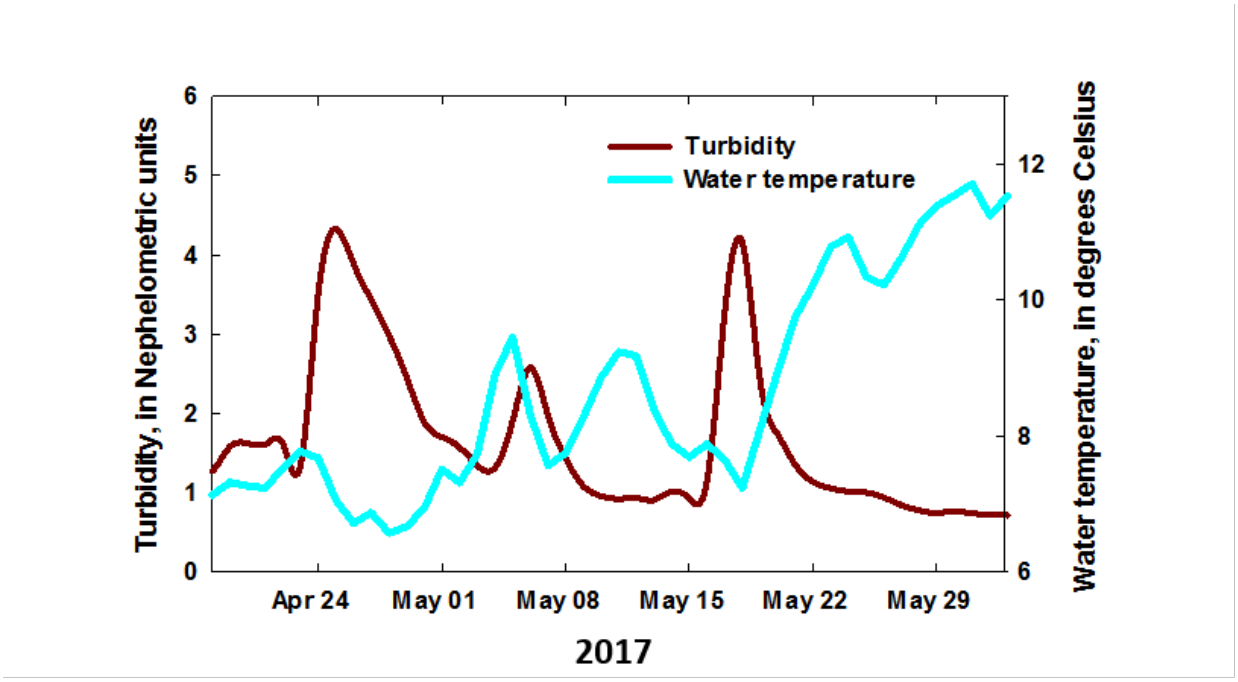

Figure 6. Graph showing turbidity and water temperature at North Fork Dam, Oregon, April 19–June 1, 2017.

Table 1. Summary statistics of hourly dam operations and environmental conditions at North Fork Dam, Oregon, April 19–June 1, 2017.

[**Abbreviations**: SD, standard deviation; ft^3/s, cubic foot per second; NTU, Nephelometric turbidity unit]

Dam operating conditions	Mean	Median	Range	SD
Project discharge (ft^3/s)	5,292.4	5,189.2	2,948.0–8,645.5	1,267.3
Spillway discharge (ft^3/s)	205.4	0	0–2394.8	509.5
Forebay elevation (feet)	664.9	664.9	664.7–665.0	0.1
Turbidity (NTUs)	1.7	1.3	0.7–4.3	1.0
Water temperature (degrees Celsius)	8.6	8.0	6.3–11.9	1.6

Fish Abundance

Data from the imaging sonar indicate that abundances of both smolt and predator-size fish near the entrance of the FSC varied as the season progressed (fig. 7). Abundance of fish observed on the imaging sonar generally were lowest during mid-April and early-May, and trended upward to a peak abundance of 5,257 fish on May 19, before decreasing again into June. Observations were dominated by smolt size fish; however, the daily abundance trends of predator-size fish generally corresponded with and followed that of the smolt-size fish.

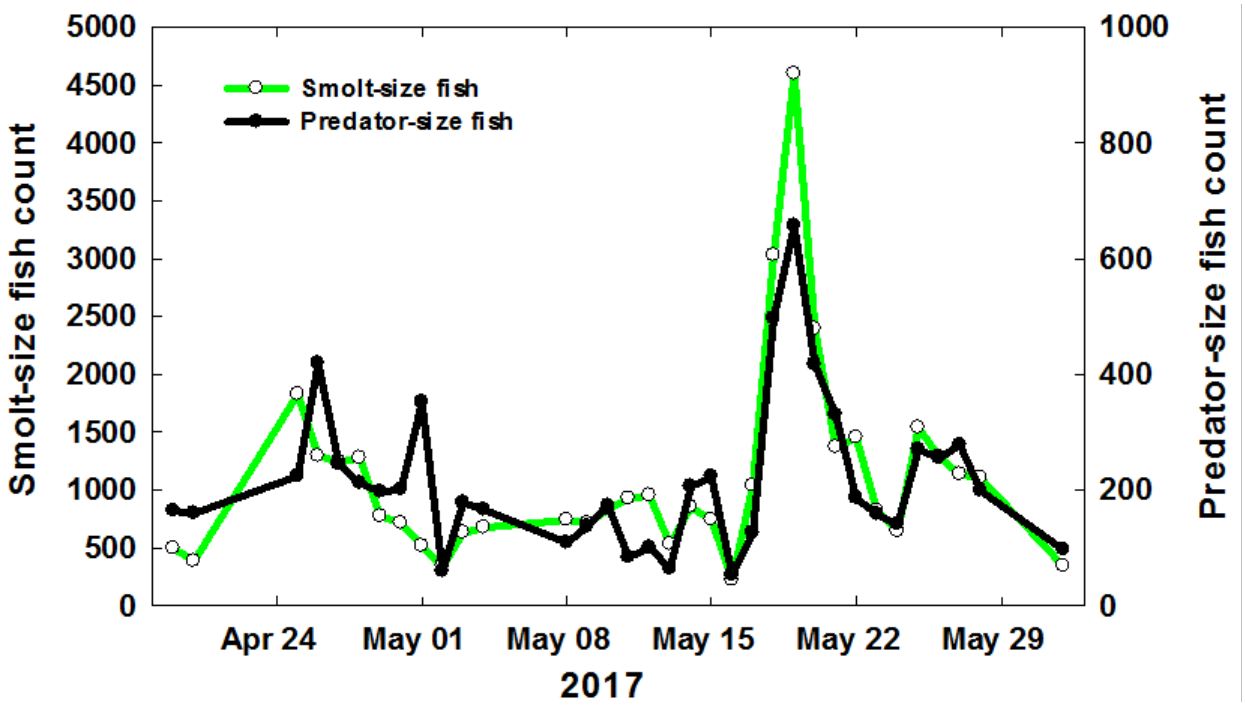

Figure 7. Graph showing daily count of fish on the date of detection using the ARIS® imaging sonar at the floating surface collector at North Fork Reservoir, Oregon, 2017.

Direction of Travel

The predominant direction of travel for fish in the acoustic beams was generally similar between the fish-size groups (table 2). Smolt-size fish observed with the imaging sonar had travel paths that were generally circular (fig. 8), with a significant (Rao $P<0.001$) primary direction of travel that was lateral to the entrance of the FSC and toward the dam. However, one lobe of the rose plot was directly toward the entrance of the FSC, indicating directed movement into the FSC. Predator-size fish observed with the imaging sonar had travel paths that were also circular (fig. 9), and with a significant (Rao $P<0.001$) primary direction of travel that was again lateral to the entrance of the FSC and toward the dam, but lacking directed movement into the FSC. Low concentration parameter (κ) values for both fish sizes reflect a reduced concentration of the distribution toward a mean direction.

Table 2. Mean travel directions and concentration parameter for fish observed using the ARIS® imaging sonar outside of the floating surface collector at North Fork Reservoir, Oregon, 2017.

[Headings of the imaging sonar is normalized to 0 degrees. Sample size is the number of fish observation events with the imaging sonar, not necessarily the number of individual fish, because a given fish could be observed more than once. **Abbreviations**: mm, millimeters; N, sample size; μ, mean travel direction (in degrees) of the fish; SE, standard error; κ, concentration parameter]

Fish size (mm)	*N*	μ (SE)	κ (SE)
Smolt (60–250)	37,466	151.7 (1.29)	0.33 (0.01)
Predator (350–650)	7,338	143.4 (1.92)	0.50 (0.02)

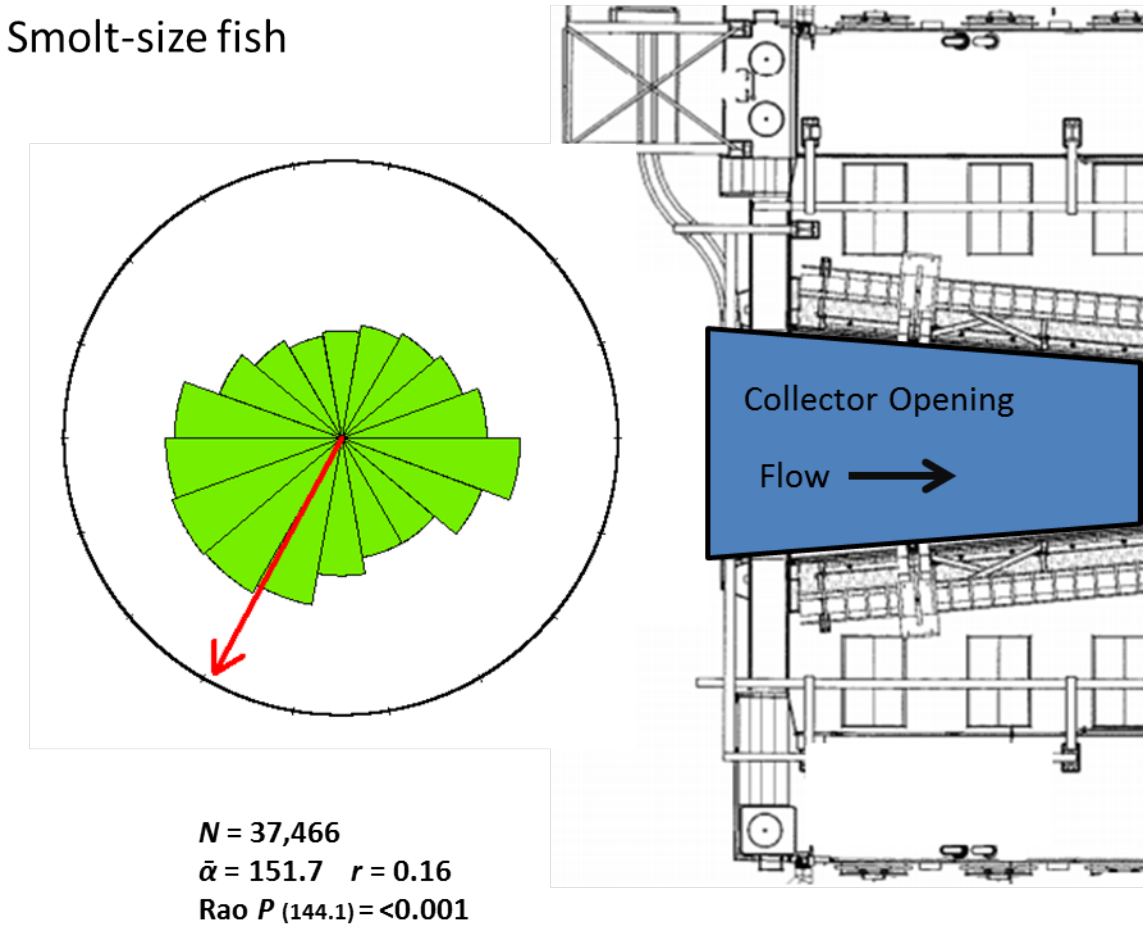

Figure 8. Rose diagram of mean travel directions (in degrees) for smolt-size fish detected using the ARIS® imaging sonar outside the floating surface collector at North Fork Reservoir, Oregon, 2017. Heading of the imaging sonar is normalized to 0 degrees (top). Sample sizes represent the number of fish (*N*) observed. Mean vector ($\bar{\alpha}$) and mean vector resultant length (*r*) are described by arrows. Rao *P* indicates significance level according to the Rao *spacing* test statistic (in parenthesis).

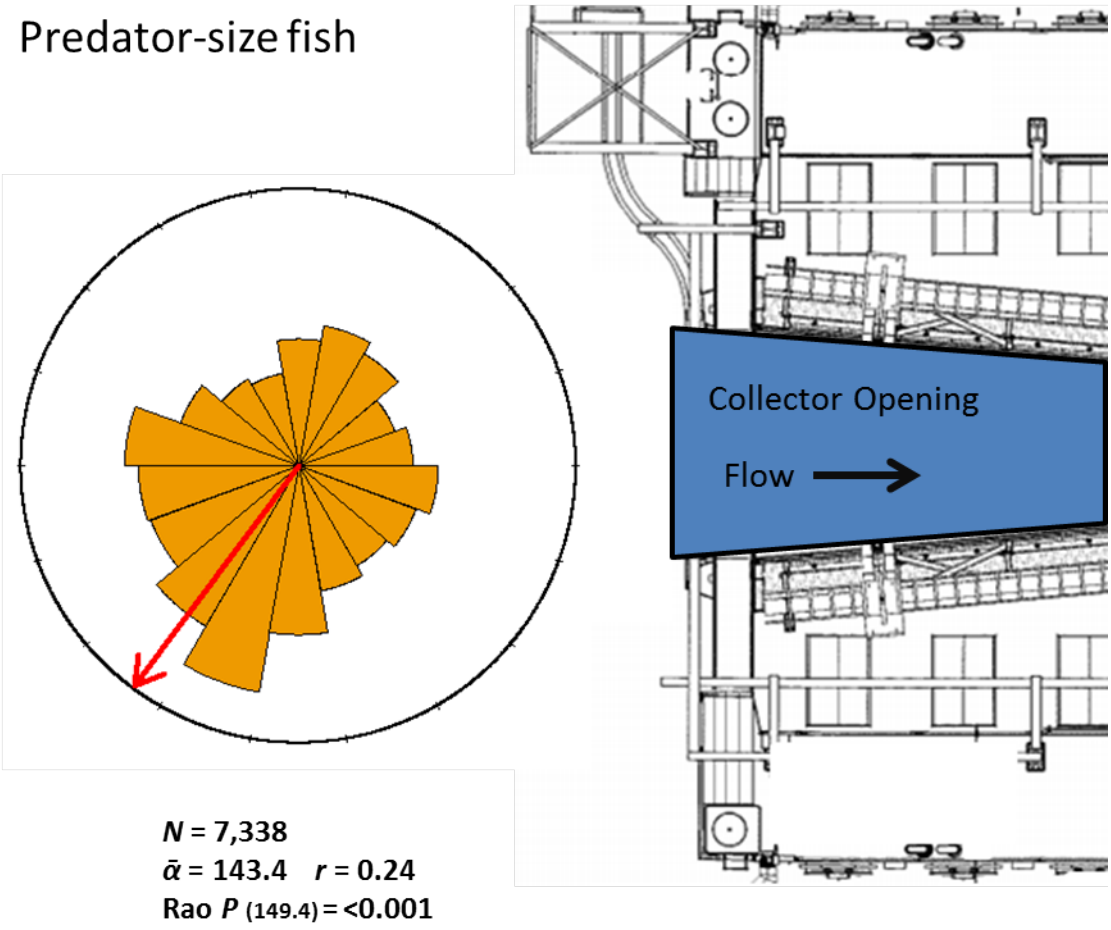

Figure 9. Rose diagram of mean travel directions (in degrees) for predator-size fish detected using the ARIS® imaging sonar outside the floating surface collector at North Fork Reservoir, Oregon, 2017. Heading of imaging sonar is normalized to 0 degrees (top). Sample sizes represent the number of fish (*N*) observed. Mean vector ($\bar{\alpha}$) and mean vector resultant length (*r*) are described by arrows. Rao *P* indicates significance level according to the Rao *spacing* test statistic (in parenthesis).

The absence of predator-size fish also influenced the count and the direction of travel of smolt-size fish near the entrance to the FSC (fig. 10). More than twice the number of smolt-size fish were observed when predator-size fish were absent (68%) compared to when predator-size fish were present (32%), and this difference was significant (X^2 [1] = 4948.4, P <0.0001). The general direction of travel (either toward or away from the FSC) was also significantly (X^2 [1] = 434.9, P <0.0001) influenced by the presence or absence of predator-size fish. When predator-size fish were absent, 52 percent of the smolt-size fish were traveling away from the entrance to the FSC, while 48 percent were traveling toward the FSC. When predator-size fish were present, a higher proportion of smolt-size fish were traveling away from the FSC (64%) than toward the FSC (36%).

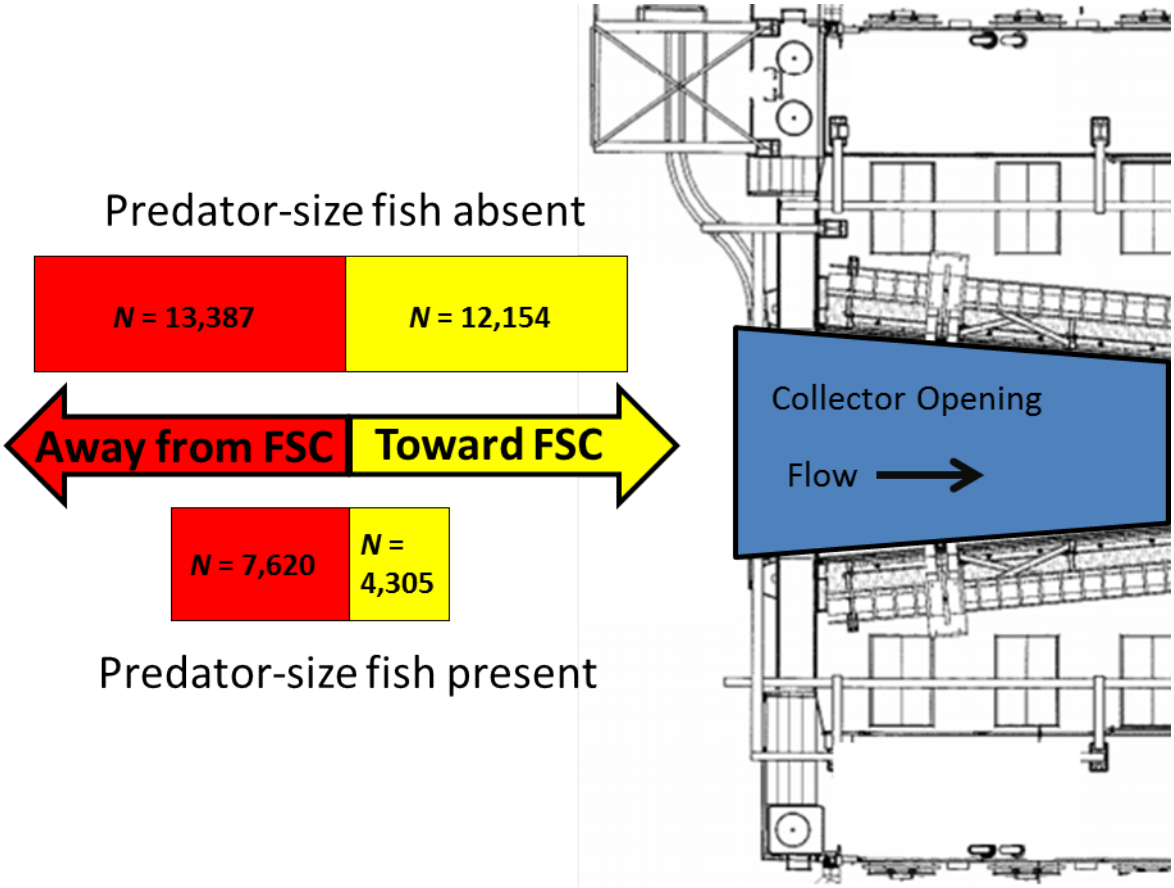

Figure 10. Diagram of directional travel for smolt-size fish detected in the presence or absence of predator-size fish using the ARIS® imaging sonar outside the floating surface collector at North Fork Reservoir, Oregon, 2017. Sample sizes represent the number of smolt-size fish (*N*) observed.

Fish Tortuosity and Swimming Velocity

The tortuosity index indicated that the tracks of fish observed near the FSC entrance differed depending on fish size (table 3; fig. 11). Tracks of smolt-size fish were more linear, with a mean tortuosity index of 1.99 (interquartile range [IQR]=0.85), whereas the tracks of predator-size fish had a mean tortuosity index that was greater (2.67, IQR=1.47). These differences were significant between fish sizes (ANOVA; $F_{1, 44,802}$=430.1, P<0.001). Smolt-size fish observed with the imaging sonar traveled with straighter tracks than predator-size fish, indicating that predator-size fish were showing greater milling behavior near the entrance to the FSC whereas smolt-size fish had more directed movement.

The speed at which fish traveled in the area upstream of the FSC also differed between the two fish-size classes (table 3; fig. 11). For example, the mean swimming velocity of smolt-size fish was 0.15 m/s (IQR=0.11) and 0.21m/s (IQR=0.13) for predator-size fish. These differences in fish swimming speed were significant between fish sizes (ANOVA; $F_{1, 44,802}$=2,470, P<0.001). These results are not surprising, as larger fish generally exhibit greater swimming abilities (Webb, 1995; Mesa and others, 2004).

Table 3. Summary statistics for the tortuosity and swimming velocity of fish observed using the ARIS® imaging sonar outside the floating surface collector at North Fork Reservoir, Oregon, 2017.

[Sample size is the number of fish observation events with the imaging sonars, not necessarily the number of individual fish, because a given fish could be observed more than once. **Abbreviations**: mm, millimeter; *N*, sample size; SD, standard deviation; IQR, interquartile range; m/s, meter per second; <, less than]

Fish size (mm)	*N*	Mean	SD	IQR	Minimum	25th percentile	50th percentile	75th percentile	Maximum
Tortuosity index									
Smolt (60–250)	37,466	1.99	2.33	0.85	1.00	1.09	1.30	1.94	77.88
Predator (350–650)	7,338	2.67	3.56	1.47	1.00	1.24	1.64	2.72	115.11
Swimming velocity (m/s)									
Smolt (60–250)	37,466	0.15	0.09	0.11	<0.01	0.09	0.13	0.19	1.82
Predator (350–650)	7,338	0.21	0.12	0.13	<0.01	0.13	0.19	0.27	1.59

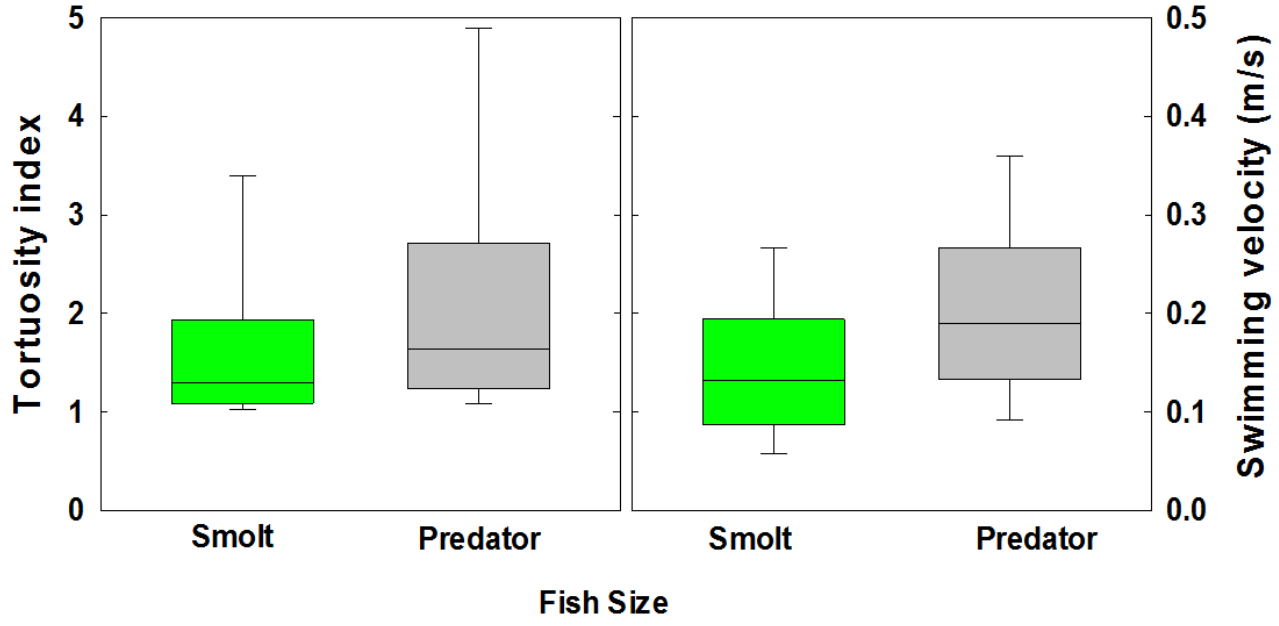

Figure 11. Boxplots of the tortuosity index and swimming velocity of fish observed with ARIS® imaging sonar near the entrance to the floating surface collector in the North Fork Reservoir, 2017. Boxes range from the 25th to the 75th percentiles, with lines indicating the medians and whiskers representing 10th and 90th percentiles.

Timing of Detection

The counts of fish observed with the imaging sonar near the entrance to the FSC differed by time and fish size (fig. 12). For predator-size fish, counts were lowest during periods of darkness and increased throughout the daylight hours until 4:00 p.m. Following 4:00 p.m., counts of predator-size fish gradually decrease along with decreasing light down to nighttime levels.

The counts of smolt-size fish show more timing variability than that of predator-size fish (fig. 12). Detections for smolt-size fish were intermediate during the nighttime hours, before falling to their lowest counts during 6:00–9:00 a.m. Detections of smolt-size fish then rose through the daytime hours before reaching a maximum count of about 3,000 fish at 4:00 p.m. In early evening (5:00–7:00 p.m.), detections again decreased, immediately following the time period when predator-size fish incidence was elevated.

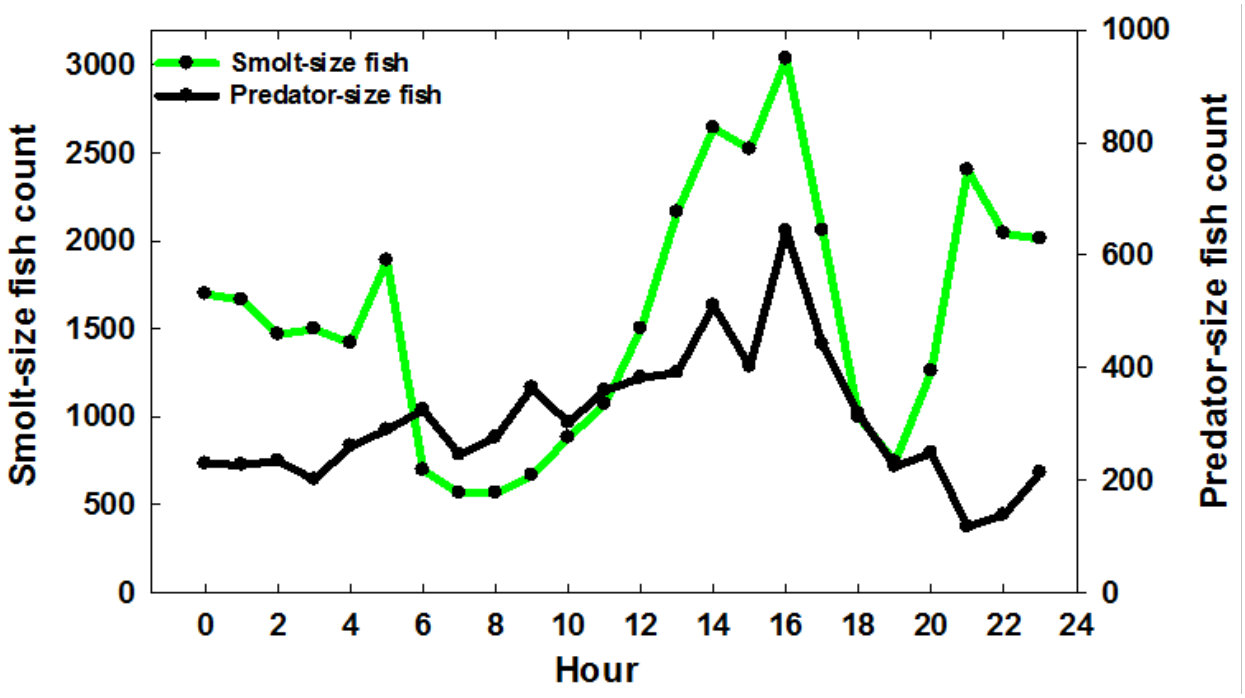

Figure 12. Graph showing count of fish by hour of detection using the ARIS® imaging sonar at the floating surface collector at North Fork Reservoir, Oregon, April 19–June 1, 2017.

Spatial Fish Distribution

The spatial distributions of fish positions near the entrance of the FSC were similar for both smolt and predator-size fish. The fish location point density data includes nearly 1.25 million location points from 44,804 individual tracks that were recorded by the imaging sonar. Observations showed that fish positions were primarily spread across the entire width of the FSC entrance, with the greatest concentrations of positions within 1–4 m from the entrance, and nearer to the dam-side of the entrance for both smolt and predator-size fish (figs. 13 and 14, respectively).

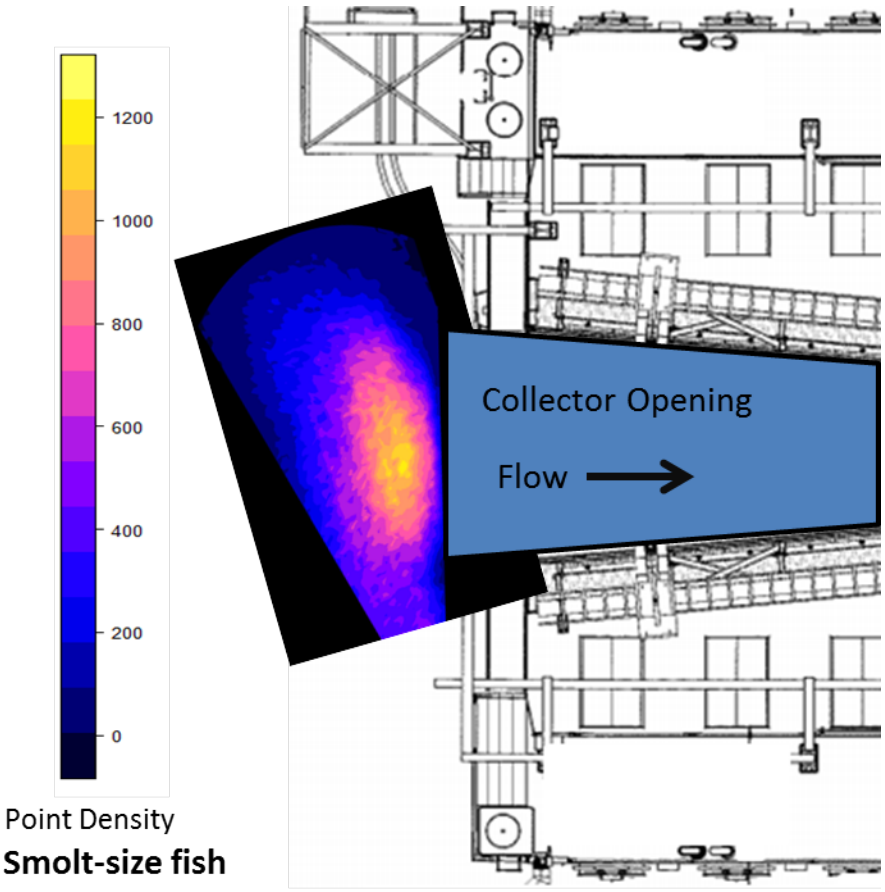

Figure 13. Graph showing the location point density for smolt-size fish detected using the ARIS® imaging sonar outside of the entrance to the floating surface collector at North Fork Reservoir, Oregon, April 19–June 1, 2017.

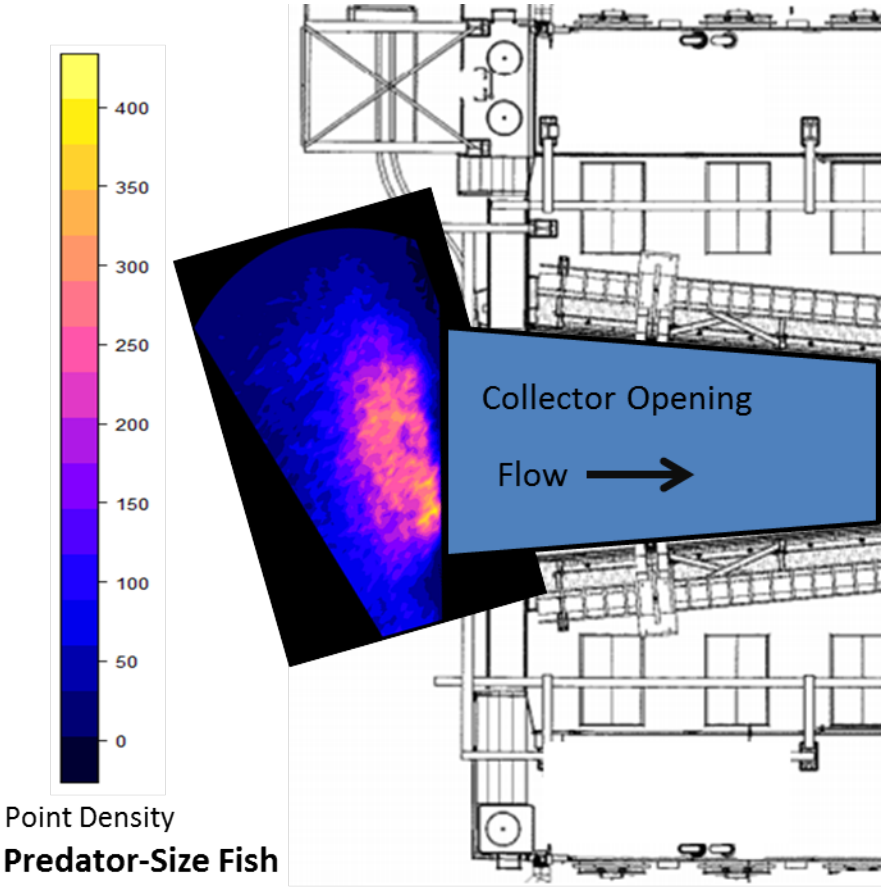

Figure 14. Graph showing the location point density for predator-size fish detected using the ARIS® imaging sonar outside of the entrance to the floating surface collector at North Fork Reservoir, Oregon, April 19–June 1, 2017.

Model Selection and Fit

Model comparison among the zero-inflation models supported including two of the four covariates (model 4; table 4). River flow and turbidity had equivocal effects on the probability of observing a zero, and thus, the absence of predator-size fish in front of the FSC. Clearly, the most important variable in determining the absence of predator-size fish was the hourly number of smolt-size fish in front of the FSC. For example, relative to other single-covariate models for zero-inflation (table 4; models 6–9), the lower AIC value was observed when the hourly count of smolt-size fish was the sole predictor (model 5). Also, when considering the zero-inflation models that were step-wise deletions from the full model (models 2–6), the greatest increase in AIC value was when the hourly number of smolt-size fish was excluded (for example, model 5 versus 6 and model 4 versus 5).

Model comparisons supported including all covariates when estimating the hourly number of predator-size fish observed at the entrance of the FSC (table 4). For example, model 4 had a 4.3 value reduction in AIC (ΔAIC) than model 10. Similar to the zero-inflation models, the most important covariate was the hourly number of smolt-size fish. For instance, of the single-covariate count models, the model including only the hourly number of smolt-size fish had the lowest AIC=7,006, whereas the other single-covariate models all had much higher AIC values >9,137.

Goodness-of-fit diagnostics supported the conclusion that the AIC best model was well fit to the data. A regression between the observed and fitted values for the hourly counts of predator-size fish in front of the FSC resulted in an intercept that was not significantly different from zero (μ=0.052; 95% CL = -0.637, 0.741) and had a slope that was indistinguishable from 1 (μ=0.994; 95% CL = 0.943, 1.046). Application of leave-one-out cross validation indicated a mean out-of-sample difference of 0.066 (SD=8.29) in the hourly number of predator-size fish counts.

Factors Affecting the Counts of Predators

The hourly number of smolt-size fish and the photoperiod were the two primary factors affecting the number of predator-size fish in front of the FSC (table 5; fig. 15). Regardless of the photoperiod, the probability of zero-inflation, or the probability of predator-size fish being absent from in front of the FSC, declined rapidly as the number of smolt-size fish increased. The steepest decline in the probability of predator-size fish being absent was when the number of smolt-size fish tracks per hour increased from 0 to about 5 fish tracks per hour. The probability of zero-inflation during the night was about twice that measured during the day, indicating that predator-size fish were more likely to be in front of the FSC during daytime compared to nighttime (fig. 15). Likewise, the odds ratio of observing no predator-size fish during the day was 0.35 (95% CL = 0.202, 0.627), indicating the probability of observing zero predator-size fish during daytime was one-third the probability of observing zero predator-size fish during nighttime.

Covariate estimates under the count model provided further insight into how environmental and biological factors help to determine the number of predator-size fish tracks in front of the FSC. The relationship between the number of smolt and predator-size fish tracks was non-linear and positive (fig. 15). The effect of photoperiod on the number of tracks by predator-size fish in front of the FSC during the day was significantly higher compared to the number of tracks by predator-size fish during the night. Higher water turbidity was associated with higher hourly numbers of tracks by predator-size fish, whereas higher river flow was associated with a relatively small decline in hourly numbers of predator-size fish.

Table 4. Model selection results showing the model, the number of parameters, Akaike's Information Criterion, and the change in AIC from the AIC lowest model (model 2).

[**Model**: Sets are composed of covariates J, square root-transformed hourly count of smolt-size fish; P, photoperiod; T, water turbidity; and F, total flow through North Fork Dam, Oregon. **K**: Number of parameters. **AIC**: Akaike's Information Criterion. **ΔAIC**: Change in AIC from the AIC lowest model]

Model number	Model	*K*	AIC	ΔAIC
1	z(.) c(.) - Null	2	9,673.52	3,237.16
2	z(J,P,T,F) c(J,P,T,F) - Full	10	6,437.50	1.14
	Zero-inflation models			
3	z(J,P,T) c(J,P,T,F)	9	6,438.08	1.72
4	*z(J,P) c(J,P,T,F)	8	6,436.36	0.00
5	z(J) c(J,P,T,F)	7	6,447.48	11.12
6	z(.) c(J,P,T,F)	6	6,490.55	54.19
7	z(F) c(J,P,T,F)	7	6,492.52	56.17
8	z(T) c(J,P,T,F)	7	6,490.29	53.93
9	z(P) c(J,P,T,F)	7	6,492.09	55.73
	Count models			
10	z(J,P) c(J,P,T)	8	6,440.660	4.31
11	z(J,P) c(J,P)	7	6,571.734	135.38
12	z(J,P) c(J)	6	7,006.734	570.38
13	z(J,P) c(P)	6	9,137.326	2,700.97
14	z(J,P) c(T)	6	9,182.754	2,746.40
15	z(J,P) c(F)	6	9,527.718	3,091.36
16	z(J,P) c(.)	5	9,615.123	3,178.77

*Model having the lowest AIC value, representing the most parsimonious model of the set.

Table 5. Parameter estimates and summary statistics for the zero-inflation Poisson model of hourly predator-size fish counts near the entrance to the floating surface collector at North Fork Reservoir, Oregon.
[**SE**: Standard error]

Coefficient	Estimate	SE	*z*-value	*P*-value
		Zero-inflation model		
α_0 – intercept	-0.040	0.325	-0.123	0.9021
$\alpha_1 - \sqrt{smoltcount}$	-0.399	0.061	-6.542	<0.0001
α_2 – photoperiod [day]	-1.032	0.289	-3.570	0.0004
		Count model		
β_0 – intercept	1.323	0.023	56.599	<0.0001
$\beta_1 - \sqrt{smoltcount}$	0.096	0.002	54.295	<0.0001
β_2 – photoperiod [day]	0.534	0.025	21.284	<0.0001
β_3 –turbidity	0.198	0.021	9.269	<0.0001
β_4 – flow	-0.052	0.021	-2.504	0.012

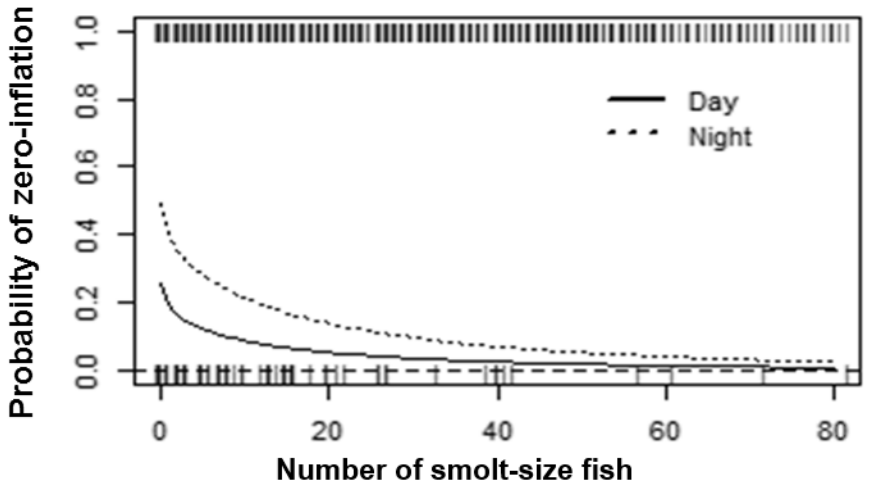

Figure 15. Graph showing the probability of zero-inflation by smolt-size fish abundance and day and night effects for the zero-inflation Poisson model of hourly predator-size fish counts near the entrance to the floating surface collector at North Fork Reservoir, Oregon. Dashed lines indicate the 95-percent confidence intervals, and the occurrence of events over the range of the covariate (number of smolt-size fish) are denoted by tick marks.

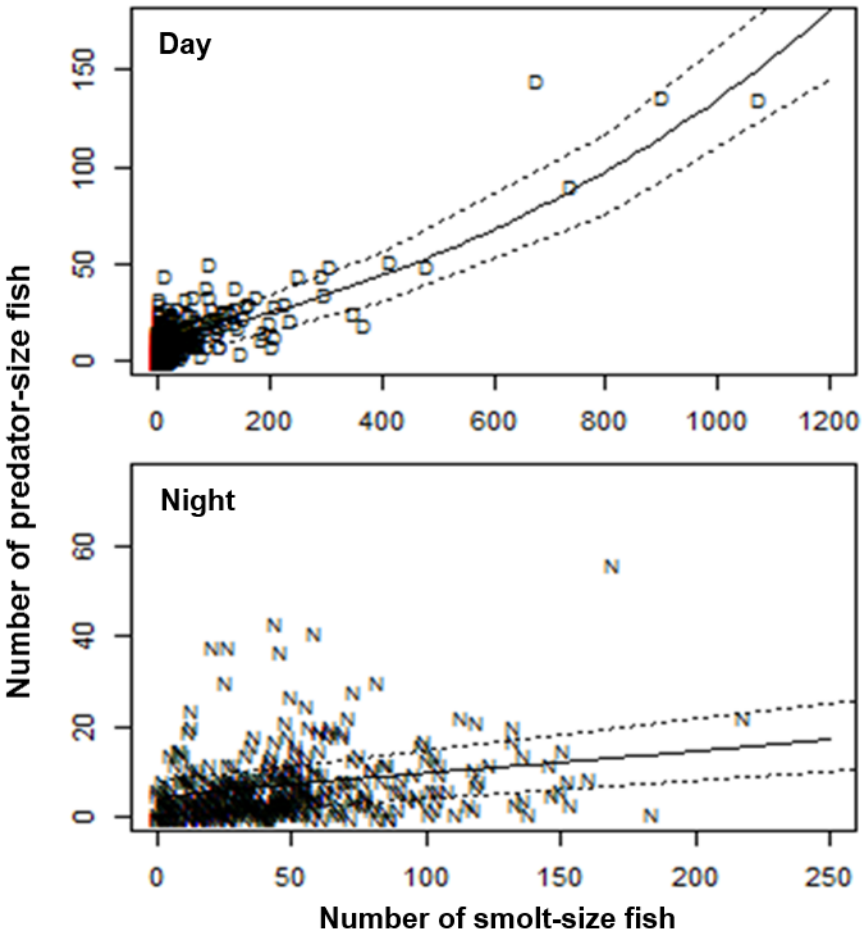

Figure 16. Graphs showing the influence of smolt-size fish abundance by day and night for the zero-inflation Poisson model of hourly predator-size fish counts near the entrance to the floating surface collector at North Fork Reservoir, Oregon. Dashed lines indicate the 95-percent confidence intervals.

Discussion

In this study, we used an imaging sonar and analytical methods to provide quantitative assessments of the abundance and movements of smolt and predator-size fish near the entrance to a FSC that was designed to capture downriver migrating salmonids. We were interested in determining the effect of potential predator-prey interactions at the FSC and how these fish were influenced by the FSC and environmental factors such as photoperiod, discharge, and water temperature. Results of this study indicate that the imaging sonar technology was capable of monitoring both smolt and predator-size fish near the FSC. This analysis enabled us to characterize fish behaviors, abundance, and movements near the FSC, and provided useful insights into potential predator and prey interactions.

The FSC at North Fork Reservoir is one of several surface-oriented collectors in use at storage and power generating dams in the Pacific Northwest (Adams and Smith, 2017). The facilities at North Fork Reservoir, along with other surface collectors, are known to have bull trout in close proximity to the entrance of the collector (McIlvaine, 2015; Beeman and others, 2016). However, bull trout typically are bottom dwellers (Scott and Crossman, 1973) and are highly substrate-oriented (Pratt, 1984), neither of which are available near the entrances to these surface collectors. The presence of these fish near the entrances to these surface collectors indicates that these structures are furnishing an attractive habitat that may be providing increased feeding opportunities for predators including bull trout and rainbow trout.

An advantage of using imaging sonars is the ability to observe untagged fish *in situ* without affecting their behavior. Therefore, this technology is well suited for evaluating the activities of fish near collection and guidance structures. However, the limitations of imaging sonars include the lack of species specificity, the possibility of counting individuals multiple times, and the difficulty in positively identifying predation attempts or success. Additionally, the time required to process the large volume of imaging sonar data into meaningful results can also be burdensome, but much of the process was automated to reduce the time required and to increase the volume of data used for analysis. In this FSC study, we assume that fish that were 60–250 mm long were salmonid smolts, that fish that were 350–650-mm long were potential predators including bull trout and rainbow trout, and that those greater than 650-mm long likely were upriver-migrating adult salmonids.

Data from the ARIS® imaging sonar indicated that increases in the daily number of observations of smolt-size fish near the entrance to the FSC generally coincided with peaks in river discharge in late April and mid-May. This is not surprising, as outmigration run timing of salmonid smolts has been found to be positively associated with increases in river flows (Petrosky and Schaller, 2010; Courter and others, 2016). We also observed similarities in the spatial use of the habitat of both smolt and predator-size fish near the entrance to the FSC. Observations for both fish size classes were primarily spread across the entire width of the FSC entrance, with the greatest concentrations occurring within 1–4 m from the entrance.

We observed behavioral differences for fish of the two size classes near the entrance to the FSC. Predator-size fish had travel paths that were generally circular, but primarily directed lateral to the entrance of the FSC and toward the dam. Smolt-size fish also had travel paths that were generally circular, but had some directed movements both toward and away from the entrance to the FSC. Also, when predator-size fish were present, overall counts of smolt-size fish were reduced and a greater proportion of smolt-size fish were observed traveling away from the FSC when predator-size fish were present. The swimming tortuosity of predator-size fish were more circuitous than that of smolt-size fish. A reduced uniform direction of travel, slow swim speed, and increased tortuosity indicate that predator-size fish may be showing greater milling behavior at the entrance to the FSC, thereby increasing the opportunity for the risk of predation of smolt-size fish. This similar milling behavior and attempted predation has been observed at other fish passage structures, while the collection or passage of predator-size fish at these structures is rare (Beeman and others, 2014, 2016; Adams and others, 2015).

There were differences in the diel abundance of the two fish size classes. For smolt-size fish, the greatest changes in abundance coincided with the crepuscular hours, with the greatest abundance observed during the afternoon hours and the lowest abundances occurring during the post-crepuscular morning hours and during the evening crepuscular period. Counts of predator-size fish were lowest during periods of darkness and gradually increased throughout the daylight hours with the greatest abundance occurring in conjunction with that of smolt-size fish in the late afternoon. Reduced abundances of predator-size fish during hours of low light suggest that the FSC is being used as a prey ambush location primarily during the daytime.

Model results indicated that the presence of smolts and environmental conditions were important determinants of the presence of predator-size fish in front of the FSC. Model parameters most important to the presence of predator-size fish were the number of tracks by smolt-size fish and photoperiod. We found that predator-size fish abundance increased near the entrance to the FSC when juvenile salmonid abundances increased, and correspondingly decreased with decreased juvenile salmonid abundances, which is similar to findings by Khan and others (2012) near a similar surface-oriented fish collector. Additionally, counts of predator-size fish in front of the FSC were much higher during the day than during the night. We measured a higher occurrence of predator-size fish tracks in front of the FSC as turbidity increased, suggesting that predators were likely increasing prey searching activity with impaired visual ability. Because these were expected results given that predator-size fish are known to be visual predators, changes in light levels and turbidity should be expected to affect the distance at which predator-prey interactions can occur and the presence and activity of predators and prey (Olla and Davis, 1990; Abrahams and Kattenfeld, 1997; Vogel and Beauchamp, 1999).

Recently, increased interest and effort has been placed on the deployment and use of forebay collectors to increase passage rates and survival of juvenile salmonids at dams. These structures capitalize on the surface-oriented behavior of outmigrating juvenile salmonids for collection; however, they also may lead to increased interactions between predators and prey by congregating fish into a small area. The imaging sonar technology used in this study proved to be an informative tool for assessing the spatial and temporal behaviors of fish near the entrance of the FSC. We were able to identify the abundance, movements, and behaviors of both smolt and predator-size fish at the entrance to the FSC. Additionally, we observed that the presence of predator-size fish negatively influenced both the abundance and behavior of smolt-size fish at the entrance to the FSC. Results of modeling potential predator-prey interactions and influences showed that the abundance of smolt-size fish primarily dictated the presence of predator-size fish near the FSC. These results can be used to help inform resource managers about abundance and behaviors of juvenile salmonids at the FSC, as well as the potential impact that the presence of predator-size fish may have on fish collection.

Acknowledgments

This study was completed with assistance from many people and organizations. Portland General Electric staff at North Fork Reservoir and Dam, especially Garth Wyatt, were instrumental in coordinating our activities, installing equipment, monitoring the imaging sonar at the floating surface collector, and reviewing this report. Our administrative and science colleagues at the Columbia River Research Laboratory (particularly Gabriel Hansen and Jesse Hall) contributed greatly to this study. This report was improved by reviews of Chris Karchesky and Philip Haner through the U.S. Geological Survey peer review program.

References Cited

Abrahams, M., and Kattenfeld, M., 1997, The role of turbidity as a constraint on predator-prey interactions in aquatic environments: Behavioral Ecology and Sociobiology, v. 40, no. 3, p. 169–174, accessed November 7, 2018, at https://doi.org/10.1007/s002650050330.

Ackerman, N.K., and Pyper, B., 2017, Evaluation of juvenile salmonid passage through the North Fork hydroelectric development, 2016 Progress Report, Clackamas River Project (FERC No. 2195) Appendix D, Article 32(b), and Appendix E, Article 32(a). Prepared by Portland General Electric, 54 p.

Ackerman, N.K., Wyatt, G., Shibahara, T., Cramer, D., David, M., and Pyper, B., 2017, Successful downstream passage of juvenile salmonids at a run-of-river hydro project in the Pacific Northwest: International Conference on Engineering and Ecohydrology for Fish Passage, 24 p.

Adams, N.S., and Smith, C.D., 2017, Spatial and temporal distribution of bull trout (*Salvelinus confluentus)*-size fish near the floating surface collector in the North Fork Reservoir, Oregon, 2016: U.S. Geological Survey Open-File Report 2017-1080, 27 p., accessed November 7, 2018, at https://doi.org/10.3133/ofr20171080.

Adams, N.S., Smith, C.D., Plumb, J.M., Hansen, G.S., and Beeman, J.W., 2015, An evaluation of fish behavior upstream of the water temperature control tower at Cougar Dam, Oregon, using acoustic cameras, 2013: U.S. Geological Survey Open-File Report 2015-1124, 62 p., accessed November 7, 2018, at https://pubs.er.usgs.gov/publication/ofr20151124.

Akaike, H., 1973, Information theory as an extension of the maximum likelihood principle, *in* Petrov, B.N., and Csaki, F., eds., Second international symposium on information theory: Budapest, Akademiai Kiado, p. 267–281.

Barrows, M.G., Davis, B., Harris, J., Bailey, E., Koski, M.L., and Starcevich, S., 2017, Clackamas River bull trout reintroduction project—2016 Annual Report: U.S. Fish and Wildlife Service and Oregon Department of Fish and Wildlife, 66 p.

Barry, P.M., Hudson, J.M., Williamson, J.D., Koski, M.L., and Clements, S.P., 2014, Clackamas River bull trout reintroduction project—2013 Annual Report: Oregon Department of Fish and Wildlife and U.S. Fish and Wildlife Service, 46 p.

Batschelet, E., 1981, Circular statistics in biology: New York, Academic Press.

Beeman, J.W., Evans, S.D., Haner, P.V., Hansel, H.C., Hansen, A.C., Hansen, G.S., Hatton, T.W., Sprando, J.M., Smith, C.D., and Adams, N.S., 2016, Evaluation of the biological and hydraulic performance of the portable floating fish collector at Cougar Reservoir and Dam, Oregon, 2014: U.S. Geological Survey Open-File Report 2016-1003, 127 p., accessed November 7, 2018, at https://pubs.er.usgs.gov/publication/ofr20161003

Beeman, J.W., Hansel, H.C., Hansen, A.C., Evans, S.D., Haner, P.V., Hatton, T.W., Kofoot, E.E., Sprando, J.M., and Smith, C.D., 2014, Behavior and dam passage of juvenile Chinook salmon at Cougar Reservoir and Dam, Oregon, March 2012–February 2013: U.S. Geological Survey Open-File Report 2014-1177, 52 p., accessed November 7, 2018, at https://pubs.usgs.gov/of/2014/1177/

Burnham, K.P., and Anderson, D.R., 2002, Model selection and multimodel inference—A practical information-theoretic approach: New York, Springer-Verlag, 488 p.

Christensen, P., and Grant, P., 2015, North Fork Dam floating surface collector hydraulic evaluation report, Clackamas River Project (FERC No. 2195): Prepared for Portland General Electric, Portland, Oregon, by R2 Resource Consultants, Inc. and Alden Research Laboratory, Inc.

Courter, I.I., Garrison, T.M., Kock, T.J., Perry, R.W., Child, D.B., and Hubble, J.D., 2016, Benefits of prescribed flows for salmon smolt survival enhancement vary longitudinally in a highly managed river system: River Research and Applications, v. 32, no. 10, p. 1999–2008, accessed November 7, 2018, at https://doi.org/10.1002/rra.3066.

Federal Energy Regulatory Commission, 2006, Final environmental impact statement for the Clackamas River Hydroelectric Project, Clackamas County, Oregon (FERC Project No. 2195): Federal Energy Regulatory Commission, 216 p.

Johnson, R.L., and Moursund, R.A., 2000, Evaluation of juvenile salmon behavior at Bonneville Dam, Columbia River, using a multibeam technique: Aquatic Living Resources, v. 13, no. 5, p. 313–318, accessed November 7, 2018, at https://doi.org/10.1016/S0990-7440(00)01088-3.

Kang, M., 2011, Semiautomated analysis of data from an imaging sonar for fish counting, sizing, and tracking in a post-processing application: Fisheries and Aquatic Sciences, v. 14, no. 3, p. 218–225, https://doi.org/10.5657/FAS.2011.0218.

Khan, F., Johnson, G.E., Royer, I.M., Phillips, N.R., Hughes, J.S., Fischer, E.S., Ham, K.D., and Ploskey, G.R., 2012, Acoustic imaging evaluation of juvenile salmonid behavior in the immediate forebay of the water temperature control tower at Cougar Dam, 2010: Pacific Northwest National Laboratory report PNNL-20625, 50 p.

Mardia, K.V., and Jupp, P.E., 2000, Directional statistics: Chichester, United Kingdom, Wiley, 492 p.

McIlvaine, P., 2015, Application review for low impact hydropower institute re-certification of the Pelton-Round Butte Project No. 2030: Wright-Pierce, 27 p., accessed November 7, 2018, at http://lowimpacthydro.org/wp-content/uploads/2007/03/Pelton-Round-Butte-Final-Report-Sept-2015.pdf.

Mesa, M.G., Weiland, L.K., and Zydlewski, G.B., 2004, Critical swimming speeds of wild bull trout: Northwest Science, v. 78, p. 59–65.

National Oceanic and Atmospheric Administration, 2008, Endangered species act section 7(a)(2) consultation biological opinion and Magnuson-Stevens fishery conservation and management act essential fish habitat consultation—Consultation on the Willamette River Basin Flood Control Project: National Oceanic and Atmospheric Administration Fisheries Log Number FINWR12000/02117, June 11, 2008, 227 p., accessed November 7, 2018, at https://www.nwcouncil.org/media/15608/willamette_biop_final_part1_july_2008.pdf.

National Oceanic and Atmospheric Administration, 2018, New floating surface collector at the Baker Hydroelectric Project is a model for innovative fish passage: National Oceanic and Atmospheric Administration, accessed November 7, 2018, at https://www.westcoast.fisheries.noaa.gov/stories/2012/2013_01_14_floating_surface_collector.html.

Olla, B.L., and Davis, M.W., 1990, Effects of physical factors on the vertical distribution of larval walleye pollock (*Theragra chalcogramma*) under controlled laboratory conditions: Marine Ecology Progress Series, v. 63, p. 105–112, https://doi.org/10.3354/meps063105.

Petrosky, C., and Schaller, H., 2010, Influence of river conditions during seaward migration and ocean conditions on survival rates of Snake River Chinook salmon and steelhead: Ecology Freshwater Fish, v. 19, no. 4, p. 520–536, https://doi.org/10.1111/j.1600-0633.2010.00425.x.

Pewsey, A., Neuhauser, M., and Ruxton, G.D., 2013, Circular statistics in R (1st ed.): Oxford, United Kingdom, Oxford University Press, 208 p.

Pratt, K.P., 1984, Habitat use and species interactions of juvenile cutthroat and bull trout in the Upper Flathead River Basin: Moscow, University of Idaho, Master's thesis, xi + 95 p.

R Core Team, 2014, R—A language and environment for statistical computing: Vienna, Austria, Foundation for Statistical Computing, accessed 2014 at http://www.R-project.org/.

Scott, W.B., and Crossman, E.J., 1973, Freshwater fishes of Canada, Bulletin 184: Ottawa, Fisheries Research Board of Canada, 966 p.

Shively, D., Allen, C., Alsbury, T., Bergamini, B., Goehring, B., Horning, T., and Strobel, B., 2007, Clackamas River bull trout reintroduction feasibility assessment—U.S. Forest Service: Sandy, Oregon, Mount Hood National Forest for the Clackamas River Bull Trout Working Group, 253 p.

Simmonds, J., and MacLennan, D., 2005, Fisheries acoustics—Theory and practice (2nd ed.): Oxford, United Kingdom, Blackwell Scientific Publications, 456 p., https://doi.org/10.1002/9780470995303.

Sweeney, C.E., Giorgi, A.E., Johnson, G.E., Hall, R., and Miller, M., 2007, Surface bypass program comprehensive review report: ENSR Corporation document number 09000-399-0409, 494 p.

U.S. Fish and Wildlife Service and Oregon Department of Fish and Wildlife, 2011, Clackamas River bull trout reintroduction implementation, monitoring, and evaluation plan: U.S. Fish and Wildlife Service, 63 p.
U.S. Geological Survey, 2018, USGS 14210000 Clackamas River at Estacada, OR: U.S. Geological Survey, National Water Information System, https://waterdata.usgs.gov/usa/nwis/uv?site_no=14210000.
Vogel, J.A., and Beauchamp, D.A., 1999, Effects of light, prey size, and turbidity on reaction distances of lake trout (*Salvelinus namaycush*) to salmonid prey: Canadian Journal of Fisheries and Aquatic Sciences, v. 56, no. 7, p. 1293–1297, https://doi.org/10.1139/f99-071.
Webb, P.W., 1995, Locomotion, *in* Groot, C., Margolis, L., and Clark, W.C., eds., Physiological ecology of Pacific salmon: Vancouver, British Columiba, Canada, University of British Columbia Press, p. 69–100.
Wyatt, G., 2017, Population level response to 21st century fish passage infrastructure: International Conference on Engineering and Ecohydrology for Fish Passage, 23 p.
Zar, J.H., 1999, Biostatistical analysis (4th ed.): Upper Saddle River, New Jersey, Prentice Hall, 663 p.
Zuur, A.F., Ieno, E.N., Walker, N.J., Saveliev, A.A., and Smith, G.M., 2009, Mixed effects models and extensions in ecology with R: New York, Springer, 574 p., https://doi.org/10.1007/978-0-387-87458-6.

Publishing support provided by the U.S. Geological Survey
Science Publishing Network, Tacoma Publishing Service Center

For more information concerning the research in this report, contact the
Director, Western Fisheries Research Center
U.S. Geological Survey
6505 NE 65th Street
Seattle, Washington 98115
https://wfrc.usgs.gov/

(online) ISSN 2331-1258
https://doi.org/10.3133/ofr20181182